Assessing the Accuracy of Contact Angle Measurements for Sessile Drops on Liquid-Repellent Surfaces

Siddarth Srinivasan,[†] Gareth H. McKinley,[*,‡] and Robert E. Cohen[*,†]

Department of Chemical Engineering, Massachusetts Institute of Technology, Cambridge MA 02139, and Department of Mechanical Engineering, Massachusetts Institute of Technology, Cambridge MA 02139

E-mail: gareth@mit.edu; recohen@mit.edu

Abstract

Gravity-induced sagging can amplify variations in goniometric measurements of the contact angles of sessile drops on super liquid-repellent surfaces. The very large value of the effective contact angle leads to increased optical noise in the drop profile near the solid-liquid free surface, and the progressive failure of simple geometric approximations. We demonstrate a systematic approach to determining the effective contact angle of drops on super-repellent surfaces. We use a perturbation solution of the Bashforth-Adams equation to estimate the contact angles of sessile drops of water, ethylene glycol and diiodomethane on an omniphobic surface using direct measurements of the maximum drop width and height. The results and analysis can be represented in terms of a dimensionless Bond number, that depends on the maximum

[*]To whom correspondence should be addressed
[†]Department of Chemical Engineering, Massachusetts Institute of Technology
[‡]Department of Mechanical Engineering, Massachusetts Institute of Technology

drop width and the capillary length of the liquid, to quantify the extent of gravity-induced sagging. Finally, we illustrate the inherent sensitivity of goniometric contact angle measurement techniques to drop dimensions as the apparent contact angle approaches 180°.

Introduction

The fabrication of low-energy, highly-textured surfaces possessing a re-entrant morphology enables liquid droplets with a range of surface tensions to exist in a non-wetting or 'Cassie-Baxter' state.[1,2] The characterization of the wetting properties of such surfaces is often carried out via the measurement of apparent contact angles at the triple phase contact line using small sessile drops placed on the surface. Experimental measurements of the contact angle of a liquid drop deposited on a textured substrate can exhibit a range of values bounded by the apparent advancing (θ^*_{adv}) and receding (θ^*_{rec}) contact angles.[3,4] There are a number of techniques to measure the contact angle of a liquid on a substrate, including optical reflectometry, contrast interferometry, the capillary rise technique, Wilhelmy plate tensiometry and various goniometric methods. The most commonly-employed technique for measuring the contact angle of drops on liquid-repellent surfaces is the sessile-drop method coupled with digital image analysis. In the sessile drop technique, a liquid drop of a known volume is gently deposited on the substrate from above and the profile of the drop is captured digitally by a high-resolution camera. A number of image analysis algorithms can be subsequently employed to estimate the contact angle from the drop profile such as polynomial fitting, spherical cap approximations[5–7] or direct fitting to numerical solutions of the Young-Laplace equation.[8–11] However, in these analysis techniques, the region in the vicinity of the triple-phase contact line can appear distorted or blurred due to optical noise caused by diffraction and scattering[12,13] leading to systematic errors in the evaluation of the tangent line.

In addition, the axial location of the base line and its contact points with the projected drop shape can be difficult to establish unambiguously, especially for highly textured surfaces,[14–17] which can lead to inconsistent determination of the apparent contact angle. The ambiguity in the measurement of contact angles due to a combination of gravity-induced drop sagging and distortion near the tangent line has recently been highlighted by Dorrer *et al.*,[14] who comment that values obtained by various Young-Laplace fitting techniques should be treated with caution, particularly for large apparent contact angles $\theta^* \approx 180^\circ$. Extrand *et al.*[17] demonstrate the deficiency of indirect geometrical measurement techniques using a hypothetical perfectly non-wetting surface and show that sagging of the contact line can lead to systematic underestimation of the true contact angles, even for relatively small drops of a few microliters in volume. Alternative capillary force measurement techniques,[18] including the Wilhemly Plate Technique,[19] are prone to potential errors arising from asymmetric coating, inaccurate determination of the periphery and irregularities in the coated substrate.[16] While there have been a number of reports on the fabrication and characterization of extreme non-wetting surfaces with an apparent contact angle $\theta^* \approx 180^\circ$,[20–24] there have been fewer studies addressing the reproducibility and sensitivity of the goniometric measurements. Zhang *et al.*[25] report variations between 156° and 173° in the contact angle of a water drop on a superhydrophobic surface fabricated by electrochemical deposition of gold clusters on a polyelectrolyte multilayer and demonstrate how different image fitting techniques can result in the aforementioned differences.[26] Variations in the contact angles of water drops on structurally-similar lithographically patterned surfaces modified by fluoropolymer treatment have been reported by different groups,[15,27] and the significant discrepancies observed have been attributed in part to differences in measurement software.[15]

In this article we quantitatively explore the inherent sensitivity of contact angle measurements to the dimensions of the sessile drop as $\theta^* \to 180^\circ$ in terms of a dimensionless Bond number (Bo) defined using the maximum drop width and the capillary length of

the liquid. We first outline the singular nature of the perturbation solution, originally developed by O'Brien,[28,29] that describes the profile of an axisymmetric sessile drop. We then demonstrate the experimental utility of this solution which enables simple measurements of the drop width and height to be used to determine, over a wide range of Bo, the apparent contact angles of water, ethylene glycol and diiodomethane drops on a spray-fabricated superoleophobic surface. The values obtained compare favorably with the values of contact angles determined from several other commonly-employed techniques. We then explore the sensitivity of the contact angle to the physical dimensions of the drop to illustrate the increasing uncertainty in the apparent contact angle θ^* as determined from the sessile drop technique as $\theta^* \to 180^\circ$.

Perturbation Approach

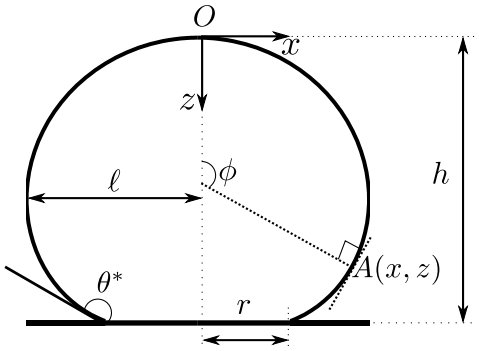

Figure 1: Schematic of an axisymmetric drop on a non-wetting substrate. For a point $A(x,z)$ on the projected drop profile, x is the lateral coordinate, z is the vertical coordinate, ϕ is the angle subtended by the normal at point A to the axis of revolution, ℓ denotes the maximum drop half-width, r is the radius of the contact line, h is the height of the drop and $\theta^* = \max(\phi)$ is the contact angle of the liquid drop at the three phase contact line.

The profile of an axisymmetric sessile drop sitting on a surface is described by the classical equation derived by Bashforth and Adams.[30]

$$\gamma_{lv}\left\{\frac{z''}{\left[1+z'^2\right]^{3/2}}+\frac{z'}{x\left[1+z'^2\right]^{1/2}}\right\}=\frac{2\gamma_{lv}}{b}+\rho g z \tag{1}$$

In this dimensional Cartesian formulation of the Young-Laplace equation applied to a point $A(x,z)$ on the projected drop profile, x is the lateral coordinate at A, z is the vertical coordinate at A, z' and z'' are the first and second derivatives of z with respect to x at A, ρ is the density of the liquid, g is the acceleration due to gravity, γ_{lv} is the surface tension of the liquid, and $b \equiv 1/z''(0)$ corresponds to the radii of curvature at the origin O which is located at the apex of the drop as seen in Figure 1. Eq. (1) is typically non-dimensionalized using a characteristic physical length scale. In the traditional formulation, Bashforth and Adams select b, the radius of curvature at the apex, as the characteristic length scale. However, the capillary length of the liquid $a = \sqrt{\gamma_{lv}/\rho g}$, has also been used to non-dimensionalize the spatial coordinates.[31,32] In both these cases, a non-dimensional Bond number can then be defined using the radius of curvature as $\beta = (\rho g b^2)/\gamma_{lv} = b^2/a^2$, and is commonly used as a dimensionless measure of the extent of gravitational forces relative to capillary forces acting on the drop. The lateral coordinate x of the point A is not a single valued function of z and it is therefore convenient to express the coordinates in a parametric form[33] using the parameter $\phi = \tan^{-1}(z'(x))$, where ϕ is the angle between the surface normal at A and the axis of revolution (Figure 1). Upon non-dimensionalizing with the capillary length $a = \sqrt{\gamma_{lv}/\rho g}$, the Bashforth-Adams equation (Eq. (1)) can be re-written as a pair of coupled first-order differential equations:

$$\frac{dX}{d\phi} = \frac{X\cos\phi}{(XZ + XP - \sin\phi)}, \quad \frac{dZ}{d\phi} = \frac{X\sin\phi}{(XZ + XP - \sin\phi)} \tag{2}$$

where the non-dimensional lateral coordinate is $X \equiv x/a$, the non-dimensional vertical coordinate is $Z \equiv z/a$ and the constant non-dimensional pressure at the apex of the drop is $P \equiv 2a/b$. The maximum value of the parametric angle ϕ is identified as the contact angle between the sessile drop and the substrate, *i.e.* $\max(\phi) = \theta^*$. The shape of the sessile drop is therefore specified by the locus of all points $A\{x(\phi),z(\phi)\}$ satisfying Eq. (2), along with the apparent contact angle θ^* between the sessile drop and the substrate. The non-dimensional volume of the liquid drop can be expressed exactly as

$V \equiv v/a^3 = \int_0^H \pi X^2 dZ = \pi R\,(RH + RP - 2\sin\theta^*)$, where $R \equiv r/a = X(\phi)|_{\phi=\theta^*}$ is the dimensionless radius of the drop at the three phase contact line and $H \equiv h/a = Z(\phi)|_{\phi=\theta^*}$ is the dimensionless height of the drop.[30]

While the Bashforth-Adams equation (Eq. (2)) does not have a closed-form analytical solution, there have been a number of attempts to determine approximate solutions through perturbation analyses[34–37] and these have been reviewed by Hometcovschi *et al*.[38] In an alternate formulation of the Bashforth-Adams equation O'Brien,[28,29] following the suggestion of Padday,[39] identifies the maximum dimensionless half-width of the drop $\epsilon \equiv \ell/a = X(\pi/2)$ as the relevant ratio of physical length scales to parametrize the effects of gravity, where ϵ can be accurately determined from imaging of the drop width 2ℓ on a liquid-repellent surface and *a priori* knowledge of the capillary length of the liquid drop. Upon rescaling the lengths with ϵ, a new Bond number, $Bo \equiv \rho g \ell^2/\gamma_{lv} = \epsilon^2$ can be defined which incorporates the physical size of the drop along with the material properties of the liquid. In Figure 2, we show the profiles of two liquid drops evaluated by numerically solving Eq. (2) with a fixed volume of $v = 5$ μL and a capillary length of $a = 1.25$ mm (typical of diiodomethane) on substrates characterized by an apparent contact angle of $\theta^* = 150^\circ$ (Figure 2(a)) and $\theta^* = 180^\circ$ (Figure 2(b)) at $Bo = 0$ (dashed line) and $Bo = 0.075$ (filled line). At $Bo = 0$ (*i.e.* in the absence of gravity) the profile of the liquid drop is described by a spherical cap. The difference between the height of the spherical cap and the height of the liquid droplet incorporating gravitational sagging is denoted by δH and the difference between the contact line radii by δR. Both δH and δR progressively increase with the apparent contact angle θ^*, leading to a systematic failure of the spherical cap approximation as the Bond number increases.[14]

An immediate consequence of scaling Eq. (2) with ϵ is the ability to seek a perturbation solution in powers of the Bond number (Bo) as the small parameter.[28,29] This formulation is readily suited to contact angle evaluation due to the ease of measuring the maximum drop width ℓ, compared to the traditional formulation of Eq. (1) which requires determi-

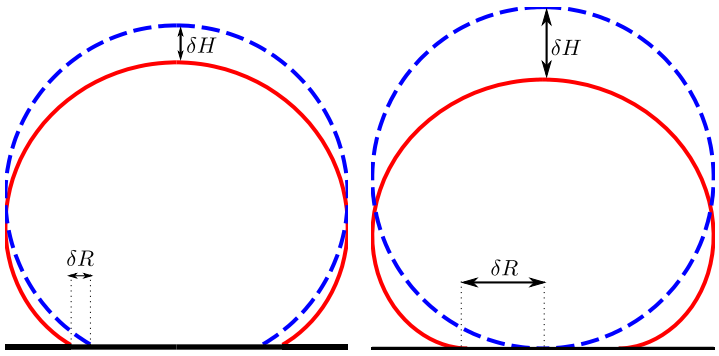

(a) $\theta^* = 150^\circ$ (b) $\theta^* = 180^\circ$

Figure 2: Numerically evaluated profiles of liquid drops of volume $v = 5$ μL and capillary length $a = 1.25$ mm ($Bo = 0.075$, filled line), where δR denotes the extent of gravity-induced sagging of the contact line from the spherical profile ($Bo = 0$, dashed line), and δH denotes displacement of the apex of the drop on substrates with an apparent contact angle of (a) $\theta^* = 150^\circ$ and (b) $\theta^* = 180^\circ$.

nation of the radius of curvature of the apex b. The singular nature of the perturbation solution can be observed qualitatively in Figure 2(b), where $dX/dZ \to \infty$ in the vicinity of the contact line as the parametric angle $\phi \to \pi$ radians, resulting in a mathematical boundary layer which necessitates a rescaling of variables in this region. O'Brien constructed a uniformly-valid perturbation solution for $0 \leq \phi \leq \pi$ by the method of matched asymptotic expansions which incorporates the presence of the boundary layer and the extent of sagging on the change in the radius of the contact line δR. The resulting expression can therefore even describe sessile drops sitting on non-wetting surfaces for which $\theta^* \approx 180^\circ$. The solution of Eq. (2) and determination of the unknown constant P (setting the capillary pressure near the apex of the drop) requires three boundary conditions, which are expressed as $X(0) = 0$, $Z(0) = 0$ and $X(\pi/2) = 1$. For completeness we provide O'Brien's composite solution below, accurate to $O(\epsilon^3)$, which we employ in this work.[40]

$$\begin{aligned} X =& \epsilon \left\{ \sin\phi - \frac{1}{2}(\pi - \phi) + \frac{1}{2}(\pi - \phi)\sqrt{1 + \frac{8\epsilon^2}{3(\pi - \phi)^2}} \right\} \\ &+ \epsilon^3 \left\{ \frac{1}{3}\cos^2\phi \tan\frac{\phi}{2} + \frac{2}{3(\pi - \phi)} \right\} + O(\epsilon^4) \end{aligned} \tag{3}$$

$$
\begin{aligned}
Z =& \epsilon \left\{ 1 - \cos\phi + \left(\frac{\pi-\phi}{2}\right)^2 - \left(\frac{\pi-\phi}{2}\right)^2 \sqrt{1 + \frac{8\epsilon^2}{3(\pi-\phi)^2}} \right\} \\
&+ \epsilon^3 \cdot \frac{1}{3} \left\{ 1 + \cos\phi - \cos^2\phi + 2\log\frac{\epsilon}{2} + 2\log\left[\sqrt{\frac{8}{3} + \frac{(\pi-\phi)^2}{\epsilon^2}} + \frac{\pi-\phi}{\epsilon} \right] \right. \\
&\left. - 2\log(\pi-\phi) + 2\log\left(\cos\frac{\phi}{2}\right) \right\} + O(\epsilon^4)
\end{aligned} \tag{4}
$$

For very small values of the scaled drop width ϵ (for which the gravitational sagging is negligible), the $O(\epsilon)$ solution as $\epsilon \to 0$ corresponds to the spherical cap given by $X^{(1)} \approx \epsilon \sin\phi$ and $Z^{(1)} \approx \epsilon(1 - \cos\phi)$, where $X^{(n)}$ and $Z^{(n)}$ correspond to the $O(\epsilon^n)$ solution as $\epsilon \to 0$. The approximate solutions expressed in Eqs. (3) and (4) are compared to the exact numerically-integrated solutions of the Bashforth-Adams equation (Eq. (2)) in Figure 3. The perturbation solutions compare well with the numerical solution for small *Bo* at all angles, but deviate increasingly as the Bond number increases. At $\phi = 0$, the deviation in the lateral coordinate given by the composite (matched) solution at $O(\epsilon^3)$ scales as $X_{\phi=0} - X^{(3)} = \Delta X \approx 4\epsilon^5/9\pi^3$, and the deviation in vertical coordinate as $Z_{\phi=0} - Z^{(3)} = \Delta Z \approx -2\epsilon^5/3\pi^2$. For sessile drops on liquid-repellent surfaces ($\theta^* \geq 90^\circ$), experimental measurements of the scaled drop half-width ϵ and drop height H allows the determination of the contact angle θ^* by numerically solving Eq. (4), while for drops with acute contact angles ($\theta^* \leq 90^\circ$) when the maximum half-width ϵ is unknown, measurements of the radius of the three phase contact line R and drop height H can be used to simultaneously solve Eqs. (3) and (4) to determine θ^*.[28,29] While knowledge of the drop volume v along with ϵ can also be used to determine the contact angle θ^*, precise measurement and control of deposited drop volumes is harder to achieve in practice.

In the following sections, we first demonstrate quantitatively the application of this technique in determining the contact angles of drops of water, diiodomethane and ethylene glycol on spray-coated liquid repellent surfaces through measurements of the drop

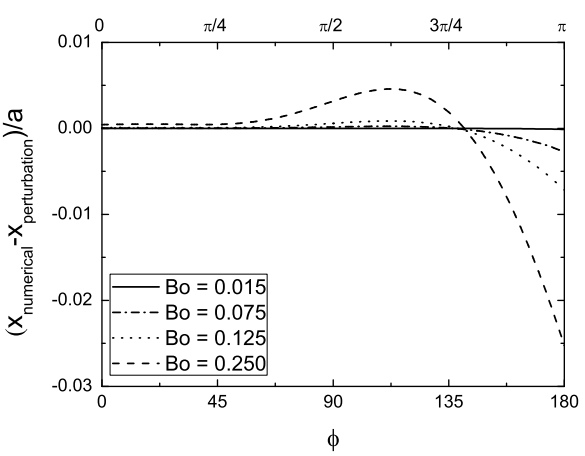

(a) Error in the lateral coordinate at $O(\epsilon^3)$ vs ϕ.

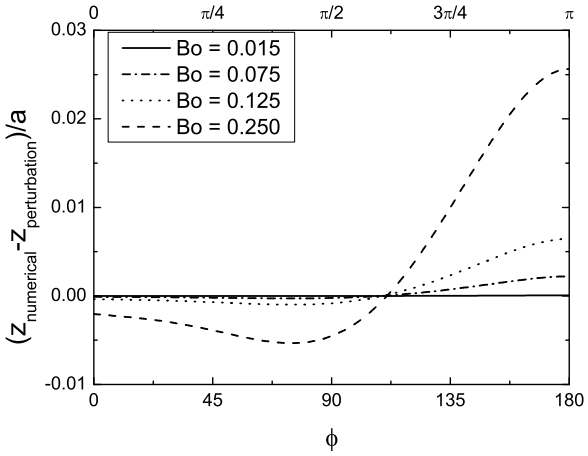

(b) Error in vertical coordinate at $O(\epsilon^3)$ vs ϕ.

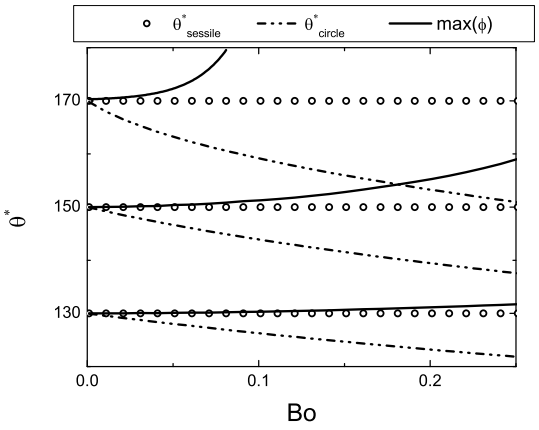

(c) Contact angle as a function of Bond number.

Figure 3: (a, b) The deviation of the approximate singular perturbation solution obtained from Eqs. (3) and (4) compared to the exact solution obtained from a numerical solver scaled by the capillary length for various Bond numbers ($Bo = \epsilon^2 = \rho g \ell^2 / \gamma_{lv}$). (c) The hypothetical effective contact angles θ^* determined using the perturbation solution (denoted $\max(\phi)$) and the spherical cap approximation (denoted θ_{circle}) as a function of Bo when compared to the true contact angle ($\theta^*_{sessile}$ from the Bashforth Adams solution).

half-width and height alone, and generate an operating diagram illustrating the sensitivity of the reported contact angles and an *a priori* error estimate as a function of the Bond number.

Methods and Materials

Poly(methyl methacrylate) (PMMA, Sigma Aldrich, $M_w = 102{,}000$ g/mol, $PDI = 1.56$) was mixed with the low surface energy molecule 1H,1H,2H,2H-heptadecafluorodecyl polyhedral oligomeric silsesquioxane (fluorodecyl POSS, $\gamma_{sv} \approx 10$ mN/m) to prepare a 50 wt% blend using the commercially-available solvent Asahiklin AK-225. A 50 mg/mL solution of the PMMA/POSS blend was sprayed with an air-brush (McMaster-Carr) on a clean flat silicon substrate at a distance of 25 cm using a pressurized nitrogen stream (170 kPa). The presence of the low surface-energy POSS molecules at the surface combined with the micro-textured corpuscular morphology produced during the spraying process confers super-liquid repellent properties to the coated substrate, which we have characterized in prior work.[41]

Contact angle measurements were performed using a ramé-hart Model 590 goniometer, after vertically dispensing droplets of deionized water, diiodomethane (Sigma-Aldrich, 99%) and ethylene glycol (Sigma-Aldrich, $\geq$ 99%) of different volumes on the spray-coated silicon substrate from above. Grayscale images were digitally captured and converted to binary 'thresholded' images, and an edge-detection operation was carried out using the freely-available ImageJ software package,[42] which implements a Sobel edge-detection algorithm to determine the drop profile from which the height h and the maximum half-width ℓ of the drop is obtained. An estimate of the contact angle $\theta^* = \max(\phi)$ can obtained from the measurement of ℓ and h by solving Eq. (4) using the 'fsolve' function from the MATLAB optimization toolbox with a trust-region algorithm (Supporting Information). We compare this estimated value of the contact angle to other commonly-

used techniques involving geometric extrapolation and curve fitting respectively. The height-width technique involves the assumption of a spherical cap, which corresponds to retaining only the $O(\epsilon)$ terms in Eq. (2) of $x \approx \ell \sin\phi$ and $z \approx \ell(1 - \cos\phi)$ in order to determine an estimate of the contact angle through the relation $\theta^*_{circ} = 2\tan^{-1}(H/R)$.[5] The commercial DropImage software provided by the goniometer manufacturer analyzes the entire drop profile and implements a curve fit of the numerical solution of the Bashforth-Adams equation to the drop profile, yielding an estimated contact angle which we denote by $\theta^*_{sessile}$.

Results and Discussion

In Figure 3(c), we compare the contact angle evaluated using the perturbation solution to that estimated from the circular approximation using various theoretical profiles which are obtained by numerically integrating the Bashforth-Adams equation for $X(\phi)$ and $Z(\phi)$ in Eq. (2) until $\phi = \theta^*_{sessile}$ (the true contact angle), which corresponds to different hypothetical non-wetting surfaces. In the absence of any gravitational sagging ($Bo = 0$), both techniques converge to $\theta^*_{sessile}$. The perturbation solution, while systematically overestimating the contact angle for large Bo due to deviations from the numerical solution, nevertheless agrees much more accurately with $\theta^*_{sessile}$ over the range of Bo shown than the commonly-used circular fit, which severely under-predicts the contact angle. It is worth noting that for a drop of a given size (or Bond number) the magnitude of the deviation becomes progressively larger as $\theta^* \to 180^\circ$; *i.e.* the sensitivity of the goniometric measurement to drop volume increases on superhydrophobic surfaces.

In Figure 4, we show the digitized profiles of sessile drops of water (Figure 4(a)) and diiodomethane (Figure 4(b)) deposited on a silicon substrate spray-coated with a 50 mg/mL solution of a 50 wt% PMMA/FluoroPOSS blend.[41] The heights of the water and diiodomethane drops are $h = 1.44$ mm and $h = 1.12$ mm, and the measured half-

widths are $\ell = 0.79$ mm and $\ell = 0.75$ mm, respectively. The appropriate Bond numbers can then be evaluated from the dimensionless maximum half-widths (ϵ) (assuming the surface tension γ_{LV} and density ρ are known) as $Bo = \epsilon^2 = \ell^2/a^2$. For the drops in Figure 4 we calculate $Bo = 0.08$ and $Bo = 0.36$ respectively. The contact angles of the liquid drops are obtained by solving Eq. (4) for ϕ numerically using the experimentally-measured values of the drop height (h) and drop width (2ℓ). The contact angle calculated for the liquid drops in Figure 4 are $\theta^* = 162^\circ$ for water, and $\theta^* = 149^\circ$ for diiodomethane. The analytical profiles of the drops as estimated from Eqs. (3) and (4) are overlaid on each of the images, and compare very well with the measured drop profile. The error in the drop height associated with deviation from the exact (numerical) Bashforth-Adams solution for the corresponding contact angle (ϕ) for each liquid is 0.4% for $Bo = 0.08$ (water) and 3.7% for $Bo = 0.36$ (diiodomethane).

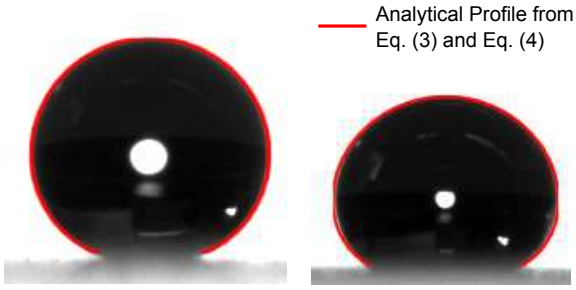

(a) Water (b) Diiodomethane

Figure 4: Liquid drops of (a) Water ($\rho = 998$ kg/m^3,$\gamma_{lv} = 72.8$ mN/m) with $v \approx 2$ μL and $\theta^* = 162^\circ$, and (b) Diiodomethane ($\rho = 3325$ kg/m^3,$\gamma_{lv} = 50.8$ mN/m) with $v \approx 1.5$ μL and $\theta^* = 149^\circ$. The drops were deposited on a silicon substrate spray-coated with a 50 mg/mL solution of 50 wt% PMMA/FluoroPOSS. The corresponding perturbation solutions (red lines) are overlaid on each of the images for Bond numbers, evaluated from the maximum drop width, of $Bo = 0.08$ and $Bo = 0.36$ respectively.

In Table 1, we list the dimensions of drops of water ($\gamma_{LV} = 72.8$ mN/m ; $\rho = 998$ kg/m^3), ethylene glycol ($\gamma_{LV} = 47.7$ mN/m ; $\rho = 1113$ kg/m^3) and diiodomethane ($\gamma_{LV} = 50.8$ mN/m ; $\rho = 3325$ kg/m^3) deposited on a flat silicon substrate that was spray-coated with a 50 mg/mL solution of 50 wt% PMMA/FluoroPOSS. The chosen liquids span a range of capillary lengths, with the high surface tension of water contributing to its large

capillary length of $a = 2.73$ mm and the high density of diiodomethane to its much smaller capillary length of 1.25 mm. Ethylene glycol, with a capillary length of 2.10 mm, is representative of other probe liquids commonly used to characterize surface wettability, whose capillary lengths typically lie between those of water and diiodomethane. The contact angle $\theta^* = \max(\phi)$ estimated by implementing O'Brien's perturbation technique compares well with the commonly used sessile drop fitting technique ($\theta^*_{sessile}$) and performs better than the circular segment approximation (θ^*_{circ}) for all three liquids. The slightly larger value of $\theta^* = \max(\phi)$ obtained from the perturbation solution is consistent with the direction of the deviation from the numerical solution seen in Figure 3(c). The observed average contact angles of water ($\theta^* = 160^\circ \pm 3^\circ$) and diiodomethane ($\theta^* = 147^\circ \pm 4^\circ$) on the spray-coated silicon substrate are consistent with previous work on characterizing its surface wettability by applying the framework of the Cassie-Baxter model.[41] Ethylene glycol, a bipolar liquid, exhibits consistently higher apparent contact angles than diiodomethane, a non-polar liquid, due to polar cohesive interactions within the liquid drop on the non-polar surface.[43]

The influence of drop volume in obtaining accurate and reproducible goniometric estimates of the contact angle has recently been discussed by Extrand and Moon.[17,44] From a theoretical perspective, the contact angle of a liquid drop contacting a substrate is a local property which is influenced by the interactions of the liquid and the surrounding vapor with the surface in the vicinity of the triple phase contact line,[4,45] and should thus be independent of the drop volume. However, during experimental measurement, larger drops are more prone to errors due to gravity-induced sagging near the contact line and deviations from a spherical shape, while smaller drops are increasingly sensitive to optical metrology errors associated with scattering, diffraction, evaporation and uncertainty in precisely locating the contact line. Direct comparison of experimental measurements with numerical solutions of the Bashforth-Adams equation does not provide a systematic insight into these uncertainties. In O'Brien's perturbation technique, the accuracy of the

Table 1: Numerical values of the drop height h, maximum half-width ℓ, dimensionless maximum half-width ϵ, Bond number Bo, drop volume v, and contact angles determined by the the three methods: the circular-segment approximation method (θ^*_{circ}), sessile drop-fitting method ($\theta^*_{sessile}$), the perturbation method ($\theta^* = \max(\phi)$). Also given is the dimensionless sensitivity of the apparent contact angle to variations in the drop height $\partial\theta^*/\partial H$ (in radians) as calculated from Eq. (5) for liquid drops on a fluorodecyl POSS spray-coated silicon substrate. The uncertainties in individual measurements of $\theta^* = \max(\phi)$ correspond to the resolution limit of the imaging camera ($\Delta h = 10$ μm), and are determined from Eq. (5) as discussed in the text.

Liquids	ϵ	Bo	h (mm)	ℓ (mm)	r (mm)	v (μL)	θ^*_{circ}	$\theta^*_{sessile}$	θ^*	$\frac{\partial\theta^*}{\partial H}$(rad)
Water										
($a = 2.73$ mm)	0.21	0.05	1.06	0.58	0.31	0.7	147°	150°	153° ± 3°	12.1
	0.29	0.08	1.44	0.79	0.38	1.9	150°	160°	162° ± 3°	16.1
	0.36	0.13	1.74	0.99	0.54	3.4	146°	155°	161° ± 3°	13.3
	0.37	0.14	1.76	1.00	0.52	3.5	147°	160°	162° ± 3°	14.9
Ethylene Glycol										
($a = 2.10$ mm)	0.24	0.06	0.93	0.50	0.25	0.5	150°	156°	162° ± 5°	17.9
	0.28	0.08	1.03	0.58	0.35	0.7	142°	152°	151° ± 3°	9.4
	0.31	0.10	1.17	0.66	0.37	1.1	145°	155°	155° ± 3°	10.4
	0.34	0.12	1.28	0.72	0.42	1.5	144°	154°	162° ± 4°	14.5
Diiodomethane										
($a = 1.25$ mm)	0.22	0.05	0.49	0.28	0.20	0.1	136°	143°	144° ± 4°	8.6
	0.29	0.08	0.63	0.36	0.26	0.2	135°	142°	149° ± 4°	8.3
	0.48	0.23	0.96	0.60	0.41	0.7	134°	146°	148° ± 3°	6.8
	0.60	0.36	1.12	0.75	0.55	1.4	128°	145°	149° ± 3°	7.6

solution is parametrized by the magnitude of Bond number Bo, which determines the extent of the deviation from the exact solution as shown in Figure 3, and sets an upper bound on the volume that should be used for a given liquid. As seen in Table 1, a volume of $v \approx 1.9$ μL for water and $v \approx 0.2$ μL for diiodomethane corresponds to a Bond number of $Bo = 0.08$ and a resulting error of $< 2\%$ in the drop height and width for a contact angle of $\theta^* = 160^\circ$. Because the capillary length of diiodomethane is smaller than water, it is more prone to sagging due to gravity and requires a correspondingly smaller volume in order to minimize deviation from the exact solution.

While the improved accuracy of the composite perturbation solution at smaller Bond numbers might initially suggest that progressively smaller drops are preferred to accurately estimate contact angles as recommended by Extrand and Moon,[17] the explicit analytical form of the composite perturbation solution allows for a quantitative estimation of the sensitivity of the experimentally determined contact angle to uncertainties in drop dimensions. In Figure 5, we have plotted contours of Eq. (4) for different Bo, which correspond to the profiles of hypothetical liquid drops of various sizes on different substrates. For a point on a given contour, the ordinate ($\theta^* = \max(\phi)$) corresponds to the contact angle of the liquid drop on that particular substrate, the abscissa ($H \equiv h/a$) corresponds to the non-dimensional height of the drop from the contact line, and the contour line itself is associated with a specific value of the Bond number, which fixes the volume of the liquid drop.

The slope of the curve $\partial\theta^*/\partial H$ describing the variation in the estimated contact angle with changes in the measured drop height then determines the uncertainty in the measured contact angle $\Delta\theta^*$ with respect to the scaled drop height ΔH via the expression $\Delta\theta^* \approx (\partial\theta^*/\partial H)\,\Delta H$. The derivative of Eq. (4)(with θ^* in radians) is given by Eq. (5):

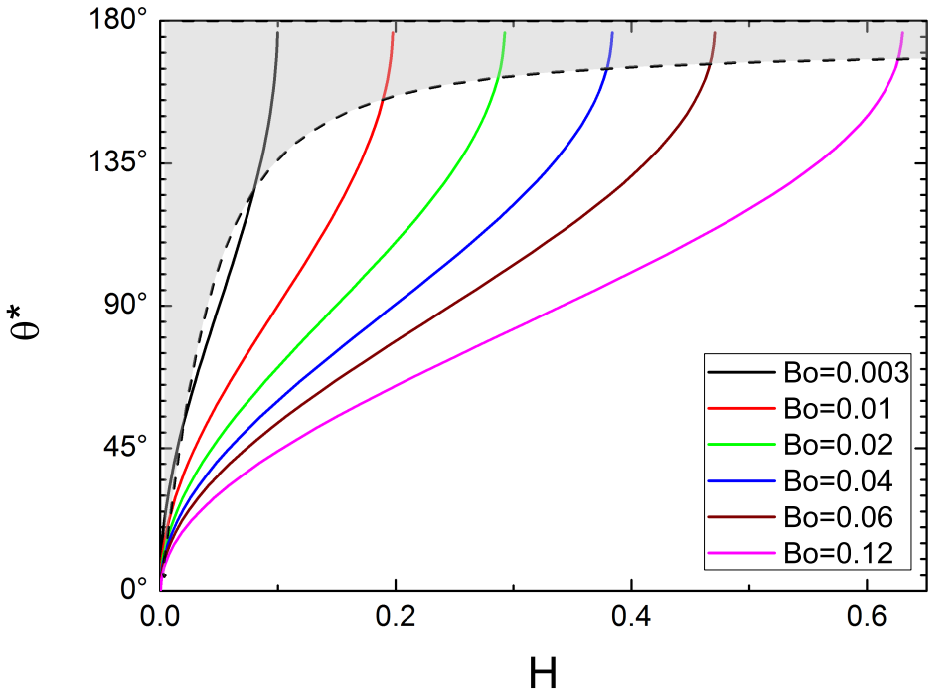

Figure 5: Contours of the contact angle θ^* evaluated from the perturbation solution as a function of the dimensionless drop height $H \equiv h/a$ for various values of the dimensionless Bond number Bo. The dashed line represents an isocline of slope $\partial\theta^*/\partial H = 25$ radians (corresponding to an uncertainty of $\Delta\theta^* = \pm 5^\circ$ for a water drop ($a = 2.73$ mm) at an imaging resolution of $\Delta h = 10$ μm). Measurements of θ^* for sessile drops in the shaded region suffer from variations larger than $\Delta\theta^*$ due to an increased sensitivity to uncertainties in imaging and establishing the base line.

$$\frac{\partial\theta^*}{\partial H} = \left\{ \frac{2\epsilon^3}{3(\pi-\theta^*)} + \frac{4\epsilon^3(\pi-\theta^*)}{8\epsilon^2 + \left[3(\pi-\theta^*) - \sqrt{24\epsilon^2 + 9(\pi-\theta^*)^2}\right](\pi-\theta^*)} \right. \\ \left. - \epsilon(\pi-\theta^*) + \epsilon\sin\theta^* - \frac{\epsilon^3}{3}\left[\sin\theta^* - \sin 2\theta^* + \tan\frac{\theta^*}{2}\right] \right\}^{-1} \tag{5}$$

The numerical values of $\partial\theta^*/\partial H$ for liquid drops deposited on the spray coated substrate in this study are also presented in Table 1. These values are used to evaluate the uncertainty of the contact angles measured using the perturbation technique that result from the resolution limit of the imaging camera ($\Delta h = 10\ \mu$m) for the various liquid drops deposited on the spray-coated substrate. For example, from the first entry in Table 1, a water drop with $Bo = 0.05$ and an apparent contact angle $\theta^* = \max(\phi) = 153^\circ$, has a dimensionless sensitivity evaluated from Eq. (5) of $\partial\theta^*/\partial H = 12.1$ radians. The uncertainty in the drop height scaled by the capillary length of the water drop ($\Delta H \equiv \Delta h/a = 0.0037$) results in an uncertainty in the apparent contact angle of $\Delta\theta^* \approx (\partial\theta^*/\partial H)\,\Delta H \approx 3^\circ$. Additional ambiguities in establishing the position of the baseline will serve to amplify this value, by increasing the uncertainty in the drop height ΔH. Eq. (5) provides a systematic framework which relates the sensitivity of the apparent contact angle to uncertainties in individual measurements of drop dimensions, and allows the determination of the appropriate drop sizes (or Bond numbers) required to accurately evaluate apparent contact angles θ^* on liquid repellent surfaces.

For a specified tolerance in the contact angle ($\Delta\theta^*$) and a given level of uncertainty in the dimensionless drop height (ΔH), an isocline with a constant slope ($\partial\theta^*/\partial H \approx \Delta\theta^*/\Delta H$) demarcates the the boundary of the regime within which accurate and reproducible values of the contact angle can be measured, as illustrated in Figure 5. For the shaded region above the isocline, even a small uncertainty in measuring the drop dimensions, or the drop volume, or in specifying the base line required for curve-fitting

algorithms, can result in significant variations of the measured contact angle. The sensitivity of the apparent contact angle θ^* progressively increases with decreasing Bond number (or drop volume), which sets a lower bound on the size of the liquid drop which can be used to obtain accurate measurements of θ^*. The expression in Eq. (5) and the resulting uncertainty in the contact angle due to the uncertainty in drop height diverges in all cases as $\theta^* \to 180^\circ$, even for small Bond numbers where the perturbation solution is very accurate (as shown in Figure 3). The singular nature of the solution to the Bashforth-Adams equation is increasingly apparent in the case of extreme non-wetting surfaces. On a hypothetical non-wetting surface with a true contact angle of 179°, an uncertainty of as small as $\Delta h = 1$ μm in the measurement of the height or location of the base line for a water drop of volume $v = 1.4$ μL and surface tension $\gamma_{LV} = 72.8$ mN/m ($Bo = 0.06$) can result in an uncertainty in the contact angle of as large as $\Delta\theta^* \approx 10^\circ$. The agreement between the perturbation solution and the exact numerical solution employed by various sessile-drop fitting techniques suggest that a similar concern with contact angle sensitivity is expected as $\theta^* \to 180^\circ$ even when software that fits the digitized profile to the full Bashforth-Adams solution is employed, contributing to the large variation in contact angles observed on highly textured surfaces.[14,15,25,26] This inherent sensitivity of contact angle measurements on super-repellent substrates with apparent contact angles near 180° necessitates careful and accurate measurements of drop dimensions in this regime and the development of new, robust fitting techniques.[11,16,46]

Conclusion

The utility of O'Brien's singular perturbation solution to the Bashforth-Adams equation in determining the apparent contact angle of sessile liquid drops on super-repellent surfaces has been experimentally demonstrated. The contact angle θ^* is systematically obtained in this technique using the following algorithm:

(i) Deposit the drop on the surface vertically from above,

(ii) Precisely measure the maximum width 2ℓ and the height h of the drop,

(iii) Evaluate the dimensionless Bond number $Bo = \epsilon^2 = \rho g \ell^2 / \gamma_{LV}$ using known values of ρ and γ_{LV},

(iv) Numerically solve Eq. (4) to determine the apparent contact angle θ^* which satisfies $Z(\phi)|_{\phi=\theta^*} = H$,

(v) Calculate $(\partial\phi/\partial H)\,|_{\phi=\theta^*}$ using Eq. (5) to get a measure of the solution sensitivity and an *a priori* estimate of $\Delta\theta^*$ for a known measurement uncertainty in the dimensionless height $\Delta H = \Delta h/a$.

The contact angles θ^* evaluated using measured values of the drop width and height are consistent (to within the known uncertainties) with those obtained by fitting the full profile using numerical solutions to the Bashforth-Adams equation and are more accurate than the circular-segment approximation which consistently under-predicts the true contact angle. The dimensionless Bond number ($Bo = \epsilon^2 = \rho g \ell^2 / \gamma_{LV}$), defined in terms of the (readily measured) maximum drop width and the capillary length of the liquid, was introduced as the relevant perturbation parameter to describe the extent of gravity-induced sagging. The magnitude of Bo establishes an upper bound on the volumes of sessile droplets of different liquids to ensure contact angles can be accurately determined using this technique. The sensitivity of contact angle measurements associated with the difficulties in precisely establishing the base line and in determining the drop dimensions can also be quantified using this approach through the expression in Eq. (5). The singular nature of the perturbation solution as $\theta^* \to 180^\circ$ and the high sensitivity of the solution associated with small changes in drop height, even for very small Bo, was shown to result in a practical lower limit on the volume of drops which can be used to determine apparent contact angles on highly non-wetting surfaces.

Acknowledgement

We acknowledge financial support from the Army Research Office (ARO) through Contract W911NF-07-D-0004, as well as the Air Force Research Laboratory, Propulsion Directorate, Air Force Office of Scientific Research. We thank Prof. Michael F. Rubner, Dr. Adam Meuler, Shreerang S. Chhatre, Hyomin Lee and Jonathan DeRocher for helpful discussions during the preparation of this manuscript, and Dr. C. Extrand for encouraging us to study this problem.

Supporting Information Available

MATLAB script to determine the apparent contact angle using the perturbation technique. This material is available free of charge via the Internet at `http://pubs.acs.org/`.

Notes and References

(1) Tuteja, A.; Choi, W.; Mabry, J. M.; McKinley, G. H.; Cohen, R. E. *Proceedings of the National Academy of Sciences* **2008**, *105*, 18200–18205h.

(2) Tuteja, A.; Choi, W.; Ma, M.; Mabry, J. M.; Mazzella, S. A.; Rutledge, G. C.; McKinley, G. H.; Cohen, R. E. *Science* **2007**, *318*, 1618–1622.

(3) Strobel, M.; Lyons, C. S. *Plasma Processes and Polymers* **2011**, *8*, 8–13.

(4) Gao, L.; McCarthy, T. J. *Langmuir* **2009**, *25*, 14105–14115.

(5) Mack, G. L. *The Journal of Physical Chemistry* **1936**, *40*, 159–167.

(6) Mack, G. L.; Lee, D. A. *The Journal of Physical Chemistry* **1936**, *40*, 169–176.

(7) Yang, M.-W.; Lin, S.-Y. *Colloids and Surfaces A: Physicochemical and Engineering Aspects* **2003**, *220*, 199–210.

(8) Rotenberg, Y.; Boruvka, L.; Neumann, A. W. *Journal of Colloid and Interface Science* **1983**, *93*, 169–183.

(9) Skinner, F. K.; Rotenberg, Y.; Neumann, A. W. *Journal of Colloid and Interface Science* **1989**, *130*, 25–34.

(10) Cheng, P.; Li, D.; Boruvka, L.; Rotenberg, Y.; Neumann, A. W. *Colloids and Surfaces* **1990**, *43*, 151–167.

(11) Stalder, A. F.; Melchior, T.; Müller, M.; Sage, D.; Blu, T.; Unser, M. *Colloids and Surfaces A: Physicochemical and Engineering Aspects* **2010**, *364*, 72–81.

(12) Sobolev, V. D.; Starov, V. M.; Velarde, M. G. *Colloid Journal* **2003**, *65*, 611–614.

(13) Zuo, Y. Y.; Do, C.; Neumann, A. W. *Colloids and Surfaces A: Physicochemical and Engineering Aspects* **2007**, *299*, 109–116.

(14) Dorrer, C.; Rühe, J. *Soft Matter* **2009**, *5*, 51–61.

(15) Dorrer, C.; Rühe, J. *Langmuir* **2006**, *22*, 7652–7657.

(16) Hung, Y.-L.; Chang, Y.-Y.; Wang, M.-J.; Lin, S.-Y. *Review of Scientific Instruments* **2010**, *81*, 065105.

(17) Extrand, C. W.; Moon, S. I. *Langmuir* **2010**, *26*, 17090–17099.

(18) De Souza, E. J.; Brinkmann, M.; Mohrdieck, C.; Crosby, A.; Arzt, E. *Langmuir* **2008**, *24*, 10161–10168.

(19) Lee, Y.-L. *Langmuir* **1999**, *15*, 1796–1801.

(20) Shibuichi, S.; Onda, T.; Satoh, N.; Tsujii, K. *The Journal of Physical Chemistry* **1996**, *100*, 19512–19517.

(21) Hosono, E.; Fujihara, S.; Honma, I.; Zhou, H. *Journal of the American Chemical Society* **2005**, *127*, 13458–13459.

(22) Gao, L.; McCarthy, T. J. *Langmuir* **2006**, *22*, 2966–2967.

(23) Gao, L.; McCarthy, T. J. *Journal of the American Chemical Society* **2006**, *128*, 9052–9053.

(24) Budunoglu, H.; Yildirim, A.; Guler, M. O.; Bayindir, M. *ACS Applied Materials & Interfaces* **2011**, *3*, 539–545.

(25) Zhang, X.; Shi, F.; Yu, X.; Liu, H.; Fu, Y.; Wang, Z.; Jiang, L.; Li, X. *Journal of the American Chemical Society* **2004**, *126*, 3064–3065.

(26) Zhang, X.; Shi, F.; Niu, J.; Jiang, Y.; Wang, Z. *Journal of Materials Chemistry* **2008**, *18*, 621–633.

(27) Öner, D.; McCarthy, T. J. *Langmuir* **2000**, *16*, 7777–7782.

(28) O'Brien, S. B. G. *Journal of Fluid Mechanics* **1991**, *233*, 519–537.

(29) O'Brien, S. B. G. M.; van den Brule, B. H. A. A. *Journal of the Chemical Society, Faraday Transactions* **1991**, *87*, 1579–1583.

(30) Bashforth, F.; Adams, J. *An attempt to test the theories of capillary action by comparing the theoretical and measured forms of drops of fluid*; Cambridge University Press: Cambridge, U.K., 1883.

(31) Huh, C.; Reed, R. L. *Journal of Colloid and Interface Science* **1983**, *91*, 472–484.

(32) Kuiken, H. K. *Colloids and Surfaces* **1991**, *59*, 129–148.

(33) Concus, P. *Journal of Fluid Mechanics* **1968**, *34*, 481–495.

(34) Chesters, A. K. *Journal of Fluid Mechanics* **1977**, *81*, 609–624.

(35) Rienstra, S. W. *Journal of Engineering Mathematics* **1990**, *24*, 193–202.

(36) Shanahan, M. E. R. *Journal of Colloid and Interface Science* **1985**, *106*, 263–264.

(37) Shanahan, M. E. R. *Journal of the Chemical Society, Faraday Transactions 1: Physical Chemistry in Condensed Phases* **1982**, *78*, 2701–2710.

(38) Homentcovschi, D.; Geer, J.; Singler, T. *Acta Mechanica* **1998**, *128*, 141–171.

(39) Padday, J. F. *Philosophical Transactions of the Royal Society of London. Series A, Mathematical and Physical Sciences* **1971**, *269*, 265–293.

(40) We wish to note that a misprint in the logarithmic term $\epsilon^3 \log \epsilon^3$ in O'Brien's solution has been corrected to $\epsilon^3 \log \epsilon$.

(41) Srinivasan, S.; Chhatre, S. S.; Mabry, J. M.; Cohen, R. E.; McKinley, G. H. *Polymer* **2011**, *52*, 3209–3218.

(42) Abràmoff, M.; Magalhaes, P.; Ram, S. *Biophotonics International* **2004**, *11*, 36–42.

(43) Chhatre, S. S.; Guardado, J. O.; Moore, B. M.; Haddad, T. S.; Mabry, J. M.; McKinley, G. H.; Cohen, R. E. *ACS Applied Materials & Interfaces* **2010**, *2*, 3544–3554.

(44) Extrand, C. W.; Moon, S. I. *Langmuir* **2010**, *26*, 11815–11822.

(45) Choi, W.; Tuteja, A.; Mabry, J. M.; Cohen, R. E.; McKinley, G. H. *Journal of Colloid and Interface Science* **2009**, *339*, 208–216.

(46) Stalder, A. F.; Kulik, G.; Sage, D.; Barbieri, L.; Hoffmann, P. *Colloids and Surfaces A: Physicochemical and Engineering Aspects* **2006**, *286*, 92–103.